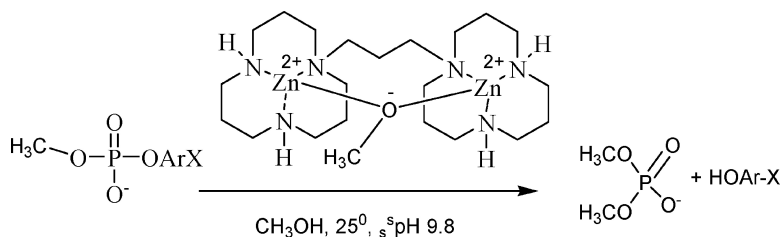


A Simple DNase Model System Comprising a Dinuclear Zn(II) Complex in Methanol Accelerates the Cleavage of a Series of Methyl Aryl Phosphate Diesters by 10⁴-10⁵

Alexei A. Neverov, C. Tony Liu, Shannon E. Bunn, David Edwards,
 Christopher J. White, Stephanie A. Melnychuk, and R. Stan Brown

J. Am. Chem. Soc., **2008**, 130 (20), 6639-6649 • DOI: 10.1021/ja8006963 • Publication Date (Web): 29 April 2008

Downloaded from <http://pubs.acs.org> on February 8, 2009



More About This Article

Additional resources and features associated with this article are available within the HTML version:

- Supporting Information
- Links to the 3 articles that cite this article, as of the time of this article download
- Access to high resolution figures
- Links to articles and content related to this article
- Copyright permission to reproduce figures and/or text from this article

[View the Full Text HTML](#)

A Simple DNase Model System Comprising a Dinuclear Zn(II) Complex in Methanol Accelerates the Cleavage of a Series of Methyl Aryl Phosphate Diesters by 10^{11} – 10^{13}

Alexei A. Neverov, C. Tony Liu, Shannon E. Bunn, David Edwards, Christopher J. White, Stephanie A. Melnychuk, and R. Stan Brown*

Department of Chemistry, Queen's University, Kingston, Ontario, Canada, K7L 3N6

Received January 28, 2008; E-mail: rsbrown@chem.queensu.ca

Abstract: The di-Zn(II) complex of 1,3-bis[N_1, N_1' -(1,5,9-triazacyclododecyl)]propane with an associated methoxide ($3:Zn(II)_2:OCH_3$) was prepared and its catalysis of the methanolysis of a series of fourteen methyl aryl phosphate diesters (**6**) was studied at pH 9.8 in methanol at 25.0 ± 0.1 °C. Plots of k_{obs} vs $[3:Zn(II)_2:OCH_3]_{free}$ for all members of **6** show saturation behavior from which K_M and k_{cat}^{max} were determined. The second order rate constants for the catalyzed reactions (k_{cat}^{max}/K_M) for each substrate are larger than the corresponding methoxide catalyzed reaction (k_2^{-OMe}) by 1.4×10^8 to 3×10^9 -fold. The values of k_{cat}^{max} for all members of **6** are between 4×10^{11} and 3×10^{13} times larger than the solution reaction at pH 9.8, with the largest accelerations being given for substrates where the departing aryloxy unit contains *ortho*-NO₂ or C(=O)OCH₃ groups. Based on the linear Brønsted plots of k_{cat}^{max} vs pK_a of the phenol, β_{lg} values of -0.57 and -0.34 are determined respectively for the catalyzed methanolysis of "regular" substrates that do not contain the *ortho*-NO₂ or C(=O)OCH₃ groups, and those substrates that do. The data are consistent with a two step mechanism for the catalyzed reaction with rate limiting formation of a catalyst-coordinated phosphorane intermediate, followed by fast loss of the aryloxy leaving group. A detailed energetics calculation indicates that the catalyst binds the transition state comprising $[CH_3O^-:6]^\ddagger$, giving a hypothetical $[3:Zn(II)_2:CH_3O^-:6]^\ddagger$ complex, by -21.4 to -24.5 kcal/mol, with the strongest binding being for those substrates having the *ortho*-NO₂ or C(=O)OCH₃ groups.

Introduction

Phosphate diesters are highly resistant toward solvolytic cleavage¹ making them ideal linking groups to be entrusted with the preservation of genetic information in RNA and DNA. Numerous enzymes are known to cleave biologically important phosphate diesters with several of these containing metal ions such as Zn²⁺, Mg²⁺, Ca²⁺, and Fe²⁺.² Because of the remarkable rate enhancements of up to 10^{17} for P–O cleavage achieved by the enzymes,³ much research has centered on the ability of small, metal containing complexes to promote the cleavage of phosphate diesters.⁴ Many of the recently reported studies have provided invaluable mechanistic information on the role by which the metal ions, in specially tailored dinuclear Zn(II) complexes,^{4a} promote the cleavage of simple RNA models such as 2-hydroxypropyl *p*-nitrophenyl phosphate (**1**),⁵ where the rate

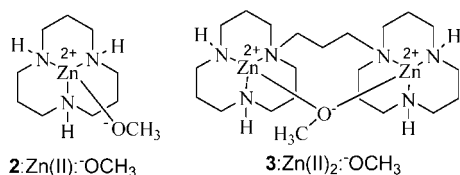
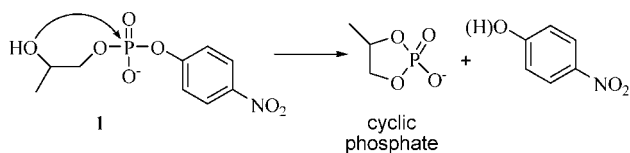
of cleavage of *p*-nitrophenoxide generally occurs with intramolecular participation of the 2-hydroxypropyl group.

In an ongoing program to investigate metal ion promoted alcoholysis of carboxylate esters and phosphate esters,⁶ we have shown that the light alcohols such as methanol and ethanol induce a remarkable enhancement of the catalysis of cleavage of **1** and related compounds by uncomplexed metal ions such as Zn²⁺ and La³⁺ as well as complexes $2:Zn(II):OCH_3$ and $3:Zn(II)_2:OCH_3$.⁸ The most recent study of the cyclization of a series of 2-hydroxypropyl aryl phosphates mediated by

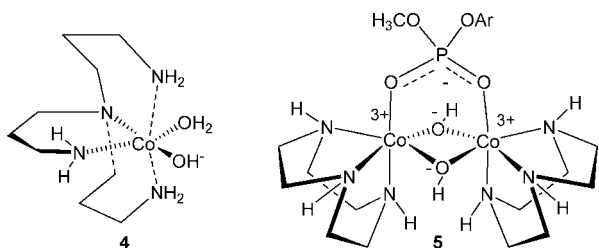
- (1) Schroeder, G. K.; Lad, C.; Wyman, P.; Williams, N. H.; Wolfenden, R. *Proc. Nat. Acad. Sci. U.S.A.* **2006**, *103*, 4052.
- (2) (a) Cowan, J. A. *Chem. Rev.* **1998**, *98*, 1067. (b) Wilcox, D. E. *Chem. Rev.* **1996**, *96*, 2435. (c) Sträter, N.; Lipscomb, W. N.; Klabunde, T.; Krebs, B. *Angew. Chem., Int. Ed. Engl.* **1996**, *35*, 2024.
- (3) Wolfenden, R.; Snider, M. J. *Acc. Chem. Res.* **2001**, *34*, 938.
- (4) For compendia of references on various metal containing complexes, see: (a) Mancin, F.; Tecilla, P. *New J. Chem.* **2007**, *31*, 800. (b) Weston, J. *Chem. Rev.* **2006**, *105*, 2151. (c) Molenveld, P.; Engbertsen, J. F. J.; Reinhoudt, D. N. *Chem. Soc. Rev.* **2000**, *29*, 75. (d) Williams, N. H.; Takasaki, B.; Wall, M.; Chin, J. *Acc. Chem. Res.* **1999**, *32*, 485. (e) Mancin, F.; Scrimin, P.; Tecilla, P.; Tonellato, U. *Chem. Commun.* **2006**, 2540. (f) Morrow, J. R.; Iranzo, O. *Curr. Opin. Chem. Biol.* **2004**, *8*, 192.

- (5) (a) Feng, G.; Mareque-Rivas, J. C.; Williams, N. H. *Chem. Commun.* **2006**, 1845. (b) Mancin, F.; Rampazzo, E.; Tecilla, P.; Tonellato, U. *Eur. J. Chem.* **2004**, 281. (c) Yang, M.-Y.; Iranzo, O.; Richard, J. P.; Morrow, J. R. *J. Am. Chem. Soc.* **2006**, *127*, 1064. (d) O'Donoghue, A. M.; Pyun, S. Y.; Yang, M.-Y.; Morrow, J. R.; Richard, J. P. *J. Am. Chem. Soc.* **2006**, *128*, 1615. (e) Iranzo, O.; Elmer, T.; Richard, J. P.; Morrow, J. R. *Inorg. Chem.* **2003**, *42*, 7737. (f) Iranzo, O.; Richard, J. P.; Morrow, J. R. *Inorg. Chem.* **2004**, *43*, 1743. (g) Iranzo, O.; Kovalevsky, A. Y.; Morrow, J. R.; Richard, J. P. *J. Am. Chem. Soc.* **2003**, *125*, 1988.
- (6) (a) Brown, R. S.; Neverov, A. J. *Chem. Soc. Perkin* **2002**, *2*, 1039. (b) Brown, R. S.; Neverov, A. A.; Tsang, J. S. W.; Gibson, G. T. T.; Montoya-Peláez, P. J. *Can. J. Chem.* **2004**, *82*, 1791. (c) Brown, R. S.; Neverov, A. A. Metal catalyzed alcoholysis reactions of carboxylate and organophosphorus esters. In *Advances in Physical Organic Chemistry*; Richard, J. P., Ed.; Elsevier: Oxford, 2007; Vol. 42, pp 271–331.
- (7) (a) Tsang, J. S.; Neverov, A. A.; Brown, R. S. *J. Am. Chem. Soc.* **2003**, *125*, 1559. (b) Neverov, A. A.; Brown, R. S. *Inorg. Chem.* **2001**, *40*, 3588. (c) Liu, C. T.; Neverov, A. A.; Brown, R. S. *Inorg. Chem.* **2007**, *46*, 1778.

$3:Zn(II)_2:OCH_3$ in methanol indicated that the transition state of the complex catalyzed reaction is stabilized by -21 to -23 kcal/mol relative to the methoxide catalyzed reaction. This stabilization energy approaches the -20 to -23 kcal/mol or so transition state stabilization energy that is seen for efficient enzymes that promote the cleavage of phosphodiester,^{1,9} bearing in mind that the solvents and substrates are different. It is apparent that the synergism between an appropriately configured dinuclear Zn(II) catalyst and the medium effect imbued by methanol accelerates these phosphoryl transfer reactions to rates greatly exceeding anything so far reported for RNA models in water.

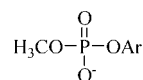


The metal ion catalyzed cleavage of phosphate diesters serving as DNA models has also seen extensive study⁴ but, due to their lower reactivity than **1**, the great bulk of the substrates studied are those with good leaving groups such as nitro- and dinitrophenoxy.¹⁰ There are some important exceptions where the reactions are reported to proceed in water with poor leaving groups,^{11,12} and there are two fine studies of the hydrolysis of a series of methyl aryl phosphates mediated by so-called ligand exchange inert complexes, namely Co(III)-tris(3-aminopropyl)-amine (**4**)¹³ and the bis[1,4,7-triazacyclononane:Co(III)(⁻OH)]₂ complex (**5**).¹⁴



As a continuation of our investigation of the catalytic ability of $3:Zn(II)_2:OCH_3$ we have studied its mediation of the methanolyses of fourteen methyl aryl phosphates (**6a–n**). The results reported herein show that all the substrates react via a mechanism involving a pre-equilibrium binding, followed by a rate limiting cleavage, where the half-times for the release of the substituted phenol (phenoxide) from the $\{3:Zn(II)_2:OCH_3:6\}$ Michaelis complex range from 0.14 s to 33 min. These correspond to accelerations for the series ranging from 4×10^{11} to 3×10^{13} relative to the background methoxide promoted

reactions for series **6** at $\text{pH } 9.8^{15}$ in methanol. In addition we report on an unusual effect where *ortho*-nitro and carbomethoxy functionalized derivatives of **6** (**6a,c,d,g,h,l**) react faster than their counterparts not having this substitution pattern, and we give a detailed energetics analysis of the catalyzed and methoxide reactions for these substrates.



- 6**
- | | |
|-------------------------------------|-----------------------------|
| a 2, 4-dinitrophenyl | h 2-nitro-4-methoxyphenyl |
| b 2-chloro-4-nitrophenyl | i 3-nitrophenyl |
| c 4-chloro-2-nitrophenyl | j 4-chlorophenyl |
| d 2-(methoxycarbonyl)-4-nitrophenyl | k 3-methoxyphenyl |
| e 2, 4, 5-trichlorophenyl | l 2-(methoxycarbonyl)phenyl |
| f 4-nitrophenyl | m phenyl |
| g 2-nitrophenyl | n 4-methoxyphenyl |

Experimental Section

Materials. Methanol (99.8% anhydrous), sodium methoxide (0.50 M solution in methanol, titrated against N/50 certified standard aqueous HCl solution and found to be 0.49 M), tetrabutylammonium hydroxide in methanol (1 M, titrated against N/50 certified standard aqueous HCl solution and found to be 1.087 M), $Zn(CF_3SO_3)_2$, 2,4-dinitrophenol (97%), 2-chloro-4-nitrophenol (97%), 4-chloro-2-nitrophenol (98%), 2,4,5-trichlorophenol (99%), 4-nitrophenol (98%), 2-nitrophenol (98%), 4-methoxy-2-nitrophenol (tech.), 4-chlorophenol (99+%), 3-nitrophenol (99%), methyl salicylate (ReagentPlus, $\geq 99\%$ GC), phenol (99%), 4-methoxyphenol (99%), 3-methoxyphenol (96%), sodium carbonate, imidazole (99%), Amberlite IR-120H ion-exchange resin (functionalized as sulfonic acid), sodium (solid in kerosene, 99%), and dimethyl phosphate (96%) were purchased from Aldrich and used without further purification. $HClO_4$ (70% aqueous solution, titrated to be 11.40 M) was purchased from Acros Organics and used as supplied. Methanol-*d*₄ was obtained from Cambridge Isotope Laboratories, Inc.

- (10) (a) Blasko, A.; Bruce, T. C. *Acc. Chem. Res.* **1999**, *32*, 475. and references therein. (b) Moss, R. A.; Park, B. D.; Scrimin, P.; Ghirlanda, G. *J. Chem. Soc., Chem. Comm.* **1996**, 1627. (c) Moss, R. A.; Zhang, J.; Bracken, K. J. *J. Chem. Soc., Chem. Comm.* **1997**, 1639. (d) Sumaoka, J.; Miyama, S.; Komiyama, M. *J. Chem. Soc., Chem. Comm.* **1994**, 1755. (e) Morrow, J. R.; Buttrey, L. A.; Shelton, V. M.; Berback, K. A. *J. Am. Chem. Soc.* **1992**, *114*, 1903. (f) Breslow, R.; Zhang, B. *J. Am. Chem. Soc.* **1994**, *116*, 7893. (g) Takeda, N.; Irisawa, M.; Komiyama, M. *J. Chem. Soc. Chem. Comm.* **1994**, 2773. (h) Hay, R. W.; Govan, N. *J. Chem. Soc., Chem. Commun.* **1990**, 714. (i) Schneider, H.-J.; Rammo, J.; Hettich, R. *Angew. Chem., Int. Ed. Engl.* **1993**, *32*, 1716. (j) Raganathan, K. G.; Schneider, H.-J. *Angew. Chem., Int. Ed. Engl.* **1996**, *35*, 1219. (k) Gómez-Tagle, P.; Yatsimirsky, A. K. *J. Chem. Soc., Dalton Trans.* **1998**, 2957. (l) Roigk, A.; Hettich, R.; Schneider, H.-J. *Inorg. Chem.* **1998**, *37*, 751. and references therein. (m) Gómez-Tagle, P.; Yatsimirski, A. K. *J. Chem. Soc., Dalton Trans.* **2001**, 2663. (n) Jurek, P. E.; Jurek, A. M.; Martell, A. E. *Inorg. Chem.* **2000**, *39*, 1016.
- (11) Jagoda, M.; Warzeska, S.; Pritzkow, H.; Wadepohl, H.; Imhof, P.; Smith, J. C.; Krämer, R. *J. Am. Chem. Soc.* **2006**, *127*, 15061.
- (12) (a) Tsubouchi, A.; Bruce, T. C. *J. Am. Chem. Soc.* **1994**, *116*, 11614. (b) Tsubouchi, A.; Bruce, T. C. *J. Am. Chem. Soc.* **1996**, *117*, 7399.
- (13) Padovani, M.; Williams, N. H.; Wyman, P. J. *Phys. Org. Chem.* **2004**, *17*, 472.
- (14) Williams, N. H.; Cheung, W.; Chin, J. J. *J. Am. Chem. Soc.* **1998**, *120*, 8079.
- (15) For the designation of pH in non-aqueous solvents, we use the forms recommended by the IUPAC, Compendium of Analytical Nomenclature. Definitive Rules 1997 3rd ed., Blackwell, Oxford, U. K. 1998. If one calibrates the measuring electrode with aqueous buffers and then measures the pH of an aqueous buffer solution, the term pH is used; if the electrode is calibrated in water and the "pH" of the neat buffered methanol solution then measured, the term pH is used; and if the electrode is calibrated in the same solvent and the "pH" reading is made, then the term pH is used. Since the autoprotolysis constant of methanol is $10^{-16.77}$, neutral pH is 8.4.

- (8) (a) Neverov, A. A.; Lu, Z.-L.; Maxwell, C. I.; Mohamed, M. F.; White, C. J.; Tsang, J. S. W.; Brown, R. S. *J. Am. Chem. Soc.* **2006**, *128*, 16398. (b) Lu, Z.-L.; Liu, C. T.; Neverov, A. A.; Brown, R. S. *J. Am. Chem. Soc.* **2007**, *129*, 11642. (c) Bunn, S. E.; Liu, C. T.; Lu, Z.-L.; Neverov, A. A.; Brown, R. S. *J. Am. Chem. Soc.* **2007**, *129*, 16238. (9) Raines, R. T. *Chem. Rev.* **1998**, *98*, 1045.

NaOCD₃ was prepared by adding sodium metal to CD₃OD; the resultant solution was titrated against certified standard aqueous HCl solution and found to be 0.502 ± 0.006 M. Lithium chloride was purchased from Anachemia Chemical LTD whereas methyl 2-hydroxy-5-nitrobenzoate (98%) was obtained from Alfa Aesar and was used as supplied. The lithium salts of all phosphate diesters (**6a–n**) were synthesized according to a general method.¹³ The lithium salts were converted into the corresponding acids by passing them through a column containing approximately 30 g of Amberlite IR-120H ion-exchange resin. Each of **6a–n** had ¹H NMR, ³¹P NMR and exact MS spectra consistent with the structure (see Supporting Information). 1,3-Bis-*N*₁-(1,5,9-triazacyclododecyl)propane (**3**) was prepared as described.¹⁶ The dinuclear **3**:Zn(II)₂:⁻OCH₃ complex was prepared as a 2.5 mM stock solution in anhydrous methanol at ambient temperature by sequential addition of aliquots of stock solutions of sodium methoxide, **3**, and Zn(CF₃SO₃)₂ such that the relative ratios were 1:1:2. This order of addition is essential for the formation of the catalyst complex which takes ~40 min in methanol (as monitored by the change in catalytic activity over time).

Methods. ¹H NMR and ³¹P NMR spectra were determined at 400 and 162.04 MHz. The CH₃OH₂⁺ concentrations were determined potentiometrically using a combination glass electrode (Radiometer model # XC100–111–120–161) calibrated with certified standard aqueous buffers (pH = 4.00 and 10.00) as described in a previous paper.¹⁷ The ³pH values in methanol were determined by subtracting the correction constant of -2.24¹⁷ from the electrode readings and the autoprotolysis constant for methanol was taken to be 10^{-16.77} M². We have found that the addition of buffers to control the ³pH inhibits the catalytic reaction, probably due to the associated counterions that bind to the catalyst, so all the kinetic studies are done under buffer free conditions although the ³pH is always found to be in the range of 9.8 ± 0.2 at the concentrations of catalyst employed.

The ³pK_a values in methanol of the corresponding phenol leaving group for **6c**, **6f**, **6i**, **6j**, **6m**, and **6n** were obtained from previous work¹⁸ and the ³pK_a values for **6a**, **6b**, and **6d** in methanol were determined by measuring the ³pH at half-neutralization with NaOMe. These values were plotted against the known ³pK_a values in water and fit by linear regression to the relationship, ³pK_a^{MeOH} = (1.08 ± 0.03)pK_a^{HOH} + (3.50 ± 0.20). This relationship was used to interpolate the ³pK_a values in methanol for the **6e**, **6h**, **6k**, and **6l** phenols. The ³pK_a values for the corresponding phenol leaving groups are listed in Table 1 along with the wavelengths at which the appearance of each product was monitored in the kinetic studies described below.

Stopped-Flow Kinetics in Methanol. The rates of the metal complex catalyzed reactions for phosphate diesters **6a–d**, **g**, and **h** were followed using an Applied Photophysics SX-17MV stopped-flow reaction analyzer with a 10 mm light path thermostated at 25.0 ± 0.1 °C. A 2.5 mM stock solution of **3**:Zn(II)₂:⁻OCH₃ in methanol was prepared in an oven-dried vial, stoppered with a needle-permitting lid and then sealed with Parafilm under nitrogen gas. After approximately 45 to 60 min (to allow the complex to form fully), portions of this were used to prepare stock catalyst solutions of concentrations ranging from 0.4 mM < [**3**:Zn(II)₂:⁻OCH₃] < 2.2 mM, which were loaded into one syringe of the stopped-flow reaction analyzer. Substrate solutions at concentrations of 8 × 10⁻⁵ M were loaded into the second syringe. After mixing, the final substrate concentration was 4 × 10⁻⁵ M. At each concentration of catalyst, five kinetic runs were recorded and the average values were used for the *k*_{obs} for appearance of phenol product vs [catalyst] plots.

Table 1. ³pK_a Values in Methanol of the Phenols Corresponding to Phosphates **6**, the λ_{cat} Wavelengths Used to Monitor the **3**:Zn(II)₂:⁻OCH₃ Catalyzed Methanolysis Reaction, and the λ_{base} Wavelengths Used to Follow the ⁻OCH₃ Promoted Methanolysis Reaction

phosphate	³ pK _a phenol	λ _{cat} (nm)	λ _{base} (nm)
6a	7.88	359	270 ^a
6b	9.35	323	395
6c	10.29	418	426
6d	10.64	345	386
6e	10.73	300	315
6f	11.18	320	400
6g	11.28	424	409
6h	11.37	291	
6i	12.41	340	387
6j	13.59	284	
6k	13.93	282	
6l	14.21	345	
6m	14.33	280	
6n	14.77	292	

^a Methoxide reaction of **6a** was monitored by following the disappearance of starting material at 270 nm. Since this process involves both aryl and P attack, the amount of each was determined from NMR analysis of the product mixture, see text.

UV-Visible Kinetics in Methanol. The rates of the **3**:Zn(II)₂:⁻OCH₃ catalyzed reactions of **6e**, **f**, and **h–n** were monitored by UV-visible spectrophotometry at 25.0 ± 0.1 °C. A 2.5 mM stock solution of **3**:Zn(II)₂:⁻OCH₃ in methanol was prepared in an oven-dried vial as above. Portions of this solution were diluted to concentrations ranging from 0.4 mM ≤ [**3**:Zn(II)₂:⁻OCH₃] ≤ 2.2 mM in anhydrous methanol inside a UV cell. The methanolysis reaction was initiated by the addition of the substrates (final concentration 4 × 10⁻⁵ M).

The methoxide catalyzed reactions of phosphates **6a–g** and **i** were also followed by UV-visible spectrophotometry at 25.0 ± 0.1 °C. Tetrabutylammonium hydroxide (TBA⁻OH; 1.087 M in methanol) was used as the base and it was assumed to be completely converted to TBA⁻OCH₃ in methanol. For each substrate, the basic reaction media were prepared in duplicate at three to five concentrations ranging from 0.02 to 0.40 M TBA⁻OCH₃ along with 0.05 or 0.1 mM of substrate in methanol. The initial rates of the reactions were obtained by fitting the first 5–10% of the abs. vs time traces by linear regression and converted to first order rate constants (*k*_{obs}) by dividing them by the expected absorbance change (ΔAbs expressed as δε/[concentration]) if the reaction were to reach 100% completion. The concentration of water at 0.02 M of TBA⁻OH in methanol was titrated (Karl Fisher) to be 46 ± 2 mM and at 0.08 M it was found to be 160 ± 10 mM. Anhydrous methanol as received was found to contain 16 ± 1 mM of water. It was assumed that the base promoted reaction was associated with methoxide and was not significantly affected by the presence of water at these concentrations.

NMR determination of reaction products. Three samples, each containing 2.5 mM of **6f** (premixed with one equivalent of NaOMe immediately before the introduction of the catalyst) and 2.5 mM of **3**:Zn(II)₂:⁻OCH₃ in 1.6 mL of anhydrous methanol, were prepared and allowed to sit at room temperature for 12 h. The reaction was then quenched by addition of two equivalents of HClO₄ (from a stock solution in methanol) to each sample. Methanol was carefully removed under vacuum and the resulting yellow oil/solid was redissolved in 800 μl of CD₃OD. ¹H NMR (400 MHz) spectra were taken for all three samples to determine the products of the reaction.

Results

Identification of Reaction Products. An ¹H NMR study was conducted with **6f** and **3**:Zn(II)₂:⁻OCH₃, 2.5 mM each in anhydrous methanol. After 12 h the reaction was quenched, the

(16) Kim, J.; Lim, H. *Bull. Korean Chem. Soc.* **1999**, *20*, 491.

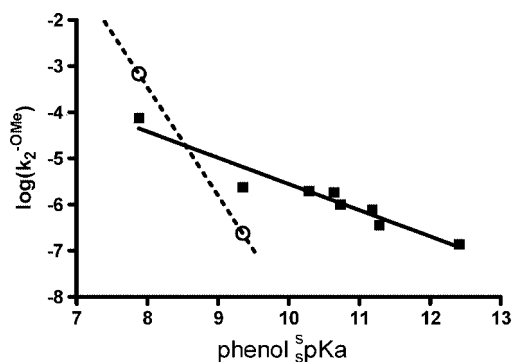
(17) Gibson, G.; Neverov, A. A.; Brown, R. S. *Can. J. Chem.* **2003**, *81*, 495.

(18) Liu, T.; Neverov, A. A.; Tsang, J. S. W.; Brown, R. S. *Org. Biomol. Chem.* **2006**, *3*, 1525.

Table 2. Second Order Rate Constants ($k_2^{-\text{OMe}}$) for the Methoxide Promoted Methanolysis of Substrates (**6a–g, i**) at $T = 25.0 \pm 0.1$ °C

phosphate	$k_2^{-\text{OMe}}$ ($\text{M}^{-1}\text{s}^{-1}$)
6a	$(7.7 \pm 0.4) \times 10^{-5a}$
6b	$(2.4 \pm 0.5) \times 10^{-6b}$
6c	$(2.0 \pm 0.1) \times 10^{-6}$
6d	$(1.9 \pm 0.1) \times 10^{-6}$
6e	$(1.0 \pm 0.1) \times 10^{-6}$
6f	$(7.9 \pm 0.6) \times 10^{-7c}$
6g	$(3.6 \pm 0.2) \times 10^{-7}$
6i	$(1.4 \pm 0.1) \times 10^{-7}$

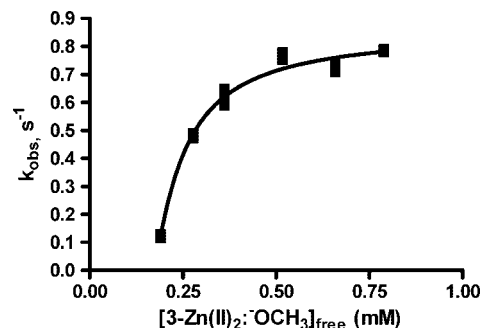
^a The $k_2^{-\text{OMe}}$ value of $(7.7 \pm 0.4) \times 10^{-5} \text{ M}^{-1} \text{ s}^{-1}$ is for attack on P to give dimethyl phosphate as the product as well as the corresponding phenoxide. Attack on the ring to give the anisole product along with methyl phosphate proceeds with a rate constant of $(6.9 \pm 0.4) \times 10^{-4} \text{ M}^{-1} \text{ s}^{-1}$. ^b The $k_2^{-\text{OMe}}$ value of $(2.4 \pm 0.5) \times 10^{-6} \text{ M}^{-1} \text{ s}^{-1}$ is for attack on P to give dimethyl phosphate as the product as well as the corresponding phenoxide. Attack on the ring to give the anisole product along with methyl phosphate proceeds with a rate constant having an upper limit of $2.4 \times 10^{-7} \text{ M}^{-1} \text{ s}^{-1}$. ^c From ref 7b.

**Figure 1.** Brønsted plot for the methoxide promoted methanolysis of phosphates (**6a–g, i**). The eight data points (■) for the base attack on the P were fit to a standard linear regression of $\log k_2^{-\text{OMe}} = (-0.57 \pm 0.06) \text{ } \text{sp}K_a + (0.14 \pm 0.68)$, $r^2 = 0.9279$. The two data points (○) for the formation of 2,4-dinitroanisole and 2-Cl-4-nitroanisole were fit to a separate standard linear regression of $\log k_2^{-\text{OMe}} = (-2.4) \text{ } \text{sp}K_a + 15.4$.

solvent removed and the residue dissolved in CD_3OD . The *p*-nitrophenol product exhibited peaks at 8.13 ppm (2H, d, *ArH*, $J = 9.09$ Hz) and 6.89 ppm (2H, d, *ArH*, $J = 9.09$ Hz). The ratio of the intensities of the *p*-nitrophenol hydrogens and those of the dimethyl phosphate product at 3.69 ppm (6H, d, *OCH*₃, $J = 10.86$ Hz) was 4:6 (see Supporting Information).

To determine whether the methoxide reaction with **6a** proceeds via attack on P or on the aryl group with formation of methyl phosphate and 2,4-dinitroanisole, a solution comprising 5 mM of **6a** and 0.2 M of NaOMe in 2 mL of anhydrous methanol was allowed to react at room temperature overnight and then, after neutralization with aqueous HCl, methanol was removed under vacuum and the residue dissolved in CD_3OD . The ¹H NMR spectrum showed a 9:1 ratio of the 2,4-dinitroanisole to 2,4-dinitrophenoxide products (see Supporting Information). The same sample was again dried under vacuum and redissolved back into anhydrous methanol for MS analysis. The TOF-EI+ MS indicated the presence of 2,4-dinitroanisole at $m/z = 198.0312$ amu [M^+], matching the calculated m/z of 198.0277 amu for $\text{C}_7\text{H}_6\text{N}_2\text{O}_5^+$.

Kinetics of Methoxide Promoted Reactions. In Table 2 are presented the second order rate constants ($k_2^{-\text{OMe}}$) for the methoxide promoted cleavage of phosphates **6a–g, i** determined at 25.0 ± 0.1 °C under pseudofirst order conditions of excess

**Figure 2.** Plot of k_{obs} vs $[\text{3:Zn(II)}_2\text{:}^-\text{OCH}_3]_{\text{free}}$ for the catalyzed methanolysis of **6c** (4×10^{-5} M) determined from the rate of appearance of product phenol at 418 nm, $\text{pH } 9.8 \pm 0.2$, and 25.0 ± 0.1 °C. Fitting the data to the expression given in eq 1 gives $K_M = (3.7 \pm 0.9) \times 10^{-4}$ M, $k_{\text{cat}}^{\text{max}} = 0.89 \pm 0.09 \text{ s}^{-1}$, and an intercept (A) = 0.174 ± 0.002 mM.

$[\text{CH}_3\text{O}^-]$ (0.02–0.08 M in methanol). Due to the slowness of the reactions, the rate constants were determined from initial rates as described above. Substrates **6j–n** reacted too slowly for reliable rate constants to be determined in a reasonable time. Because the ¹H NMR results described above indicate that ~90% of the methoxide reaction with **6a** proceeds via nucleophilic attack on the ring resulting in Ar-OP cleavage, with 10% resulting from attack on P to produce P-OAr cleavage, respective second order rate constants of $(6.9 \pm 0.4) \times 10^{-4} \text{ M}^{-1} \text{ s}^{-1}$ and $(7.7 \pm 0.4) \times 10^{-5} \text{ M}^{-1} \text{ s}^{-1}$ for each process were determined from the overall rate of disappearance of starting material at 270 nm. In the case of the second fastest substrate reacting with methoxide (**6b**), the product distribution between Ar-OP cleavage and P-OAr cleavage was determined by following both the initial rate of appearance of the phenoxide product, and the disappearance of the starting material. From the expected absorbance of phenoxide (based on the extinction coefficient at 395 nm) ~90% of the reaction generates phenoxide product, so we can estimate an upper limit for the rate constant for ring attack as $2.4 \times 10^{-7} \text{ M}^{-1} \text{ s}^{-1}$. A two-point Brønsted plot is shown in Figure 1 for the methoxide attack on the ring of the starting ester (**6a** and **6b**), $\log k_2^{-\text{OMe}} = (-2.4) \text{ } \text{sp}K_a + 15.4$. The Brønsted plot for the methoxide attack on P which is shown in Figure 1 fits a standard linear regression of $\log k_2^{-\text{OMe}} = (-0.57 \pm 0.06) \text{ } \text{sp}K_a + (0.14 \pm 0.68)$. The fit incorporates all substrates since those with an *ortho*-NO₂, Cl or carbomethoxy group fit on the same line defined by substrates without *ortho* groups.

Methanolysis of 6a–n Promoted by 3:Zn(II)₂:⁻OCH₃ in Methanol. The plots of k_{obs} for catalyzed methanolysis of **6a–n** vs $[\text{3:Zn(II)}_2\text{:}^-\text{OCH}_3]_{\text{free}}$ all exhibit saturation kinetics within the concentration range of the catalyst used for the study (see Supporting Information). Previously we established that triflate ion inhibits the catalysis afforded by $\text{3:Zn(II)}_2\text{:}^-\text{OCH}_3$ with an inhibition constant of $K_i = 14.9 \text{ mM}^{8a}$ from which one can determine the free catalyst concentration ($[\text{3:Zn(II)}_2\text{:}^-\text{OCH}_3]_{\text{free}}$) at any [triflate]. The representative plots of k_{obs} vs $[\text{3:Zn(II)}_2\text{:}^-\text{OCH}_3]_{\text{free}}$ shown in Figures 2 and 3 show that saturation kinetics were found for phosphates with both good aryloxy leaving groups (**6c**) and with poor ones (**6k**). The results for the $\text{3:Zn(II)}_2\text{:}^-\text{OCH}_3$ -catalyzed methanolysis of **6f** have been reported in an earlier study.^{8a}

Inspection of all the plots (Figures 2 and 3 and those in Supporting Information) reveals that there is a significant x-intercept which we assume results from one Zn^{2+} dissociating from the catalyst at low concentrations, and the following

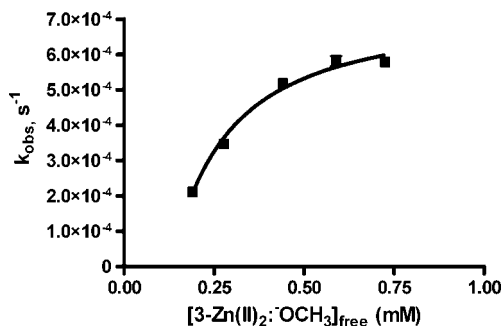


Figure 3. Plot of k_{obs} vs $[3:\text{Zn}(\text{II})_2:\text{OCH}_3]_{\text{free}}$ for the catalyzed methanolysis of **6k** (4×10^{-5} M) determined from the rate of appearance of product phenol at 282 nm, $\text{pH } 9.8 \pm 0.2$, and 25.0 ± 0.1 °C. Fitting the data to the expression given in eq 1 gives $K_M = (1.4 \pm 0.4) \times 10^{-4}$ M, $k_{\text{cat}}^{\text{max}} = (7.4 \pm 0.5) \times 10^{-4} \text{ s}^{-1}$ and an x -intercept $A = 0.13 \pm 0.01$ mM.

simplified data treatment method was devised to account for the loss of catalyst integrity at lower concentrations. For all substrates, the kinetics data in the k_{obs} vs $[3:\text{Zn}(\text{II})_2:\text{OCH}_3]_{\text{free}}$ plots were fitted to a nonlinear least-squares (NLLSQ) model given in eq 1, which is an equation that is applicable to both strong and weak binding situations:^{8a}

$$k_{\text{obs}} = k_{\text{cat}}(1 + K_B \times [S] + [\text{Cat}] \times K_B - X)/(2K_B)/[S] \quad (1)$$

where:

$$X = (1 + 2K_B \times [S] + 2 \times [\text{Cat}] \times K_B + K_B^2 \times [S]^2 - 2 \times K_B^2 \times [\text{Cat}][S] + [\text{Cat}]^2 \times K_B^2)^{0.5}$$

and K_B refers to the Cat + **6** binding constant (units of M^{-1}), the reciprocal of which is defined here as the Cat:**6** dissociation constant (K_M) in units of M. The [Cat] term in eq (1) used for the fitting corresponds to the actual concentration of *viabile* catalyst, free from triflate inhibition, which is derived according to the expression $[\text{Cat}] = ([3:\text{Zn}(\text{II})_2:\text{OCH}_3]_{\text{free}} - A)$, where A is an independently fitted parameter generally having the value ≤ 0.2 mM, corresponding to the observable intercept.

Given in Table 3 are all kinetic data determined for the $3:\text{Zn}(\text{II})_2:\text{OCH}_3$ -catalyzed methanolysis of **6a–n**, as well as the acceleration for methanolysis of the catalyst-bound substrate ($3:\text{Zn}(\text{II})_2:\text{OCH}_3:\text{6}$) relative to the background (base-promoted) reactions at $\text{pH } 9.8$. In Figure 4 is a Brønsted plot of $\log(k_{\text{cat}}^{\text{max}})$ vs $\text{p}K_a$ for all the substrates from which it is apparent that there are two lines, one for substrates having *o*-NO₂ or *o*-CO₂CH₃ groups lying above a second for all the other substrates. Linear regressions of these have respective gradients of $\beta_{\text{lg}} = -0.34 \pm 0.01$ and $\beta_{\text{lg}} = -0.59 \pm 0.03$. Also shown on the plots are two points for methyl 2-*tert*-butyl-4-nitrophenyl phosphate (Δ , $k_{\text{cat}} = 8.5 \times 10^{-4} \text{ s}^{-1}$; $\text{p}K_a = 12.03$) and dimethyl phosphate (\square , $k_{\text{cat}} = 2.2 \times 10^{-6} \text{ s}^{-1}$; $\text{p}K_a = 18.16$) which we will deal with later.

Discussion

Methoxide Reaction. The methoxide reaction for the eight most reactive substrates (**6a–g, i**) adheres to the Brønsted relationship $\log k_2^{-\text{OMe}} = (-0.57 \pm 0.06) \text{p}K_a + (0.14 \pm 0.68)$. The β_{lg} of -0.57 is at the low end of a range of -0.64 to -0.94 reported recently for the hydroxide promoted hydrolysis of methyl aryl phosphates.^{14,19} It is somewhat larger than the value of -0.35 for attack of the good nucleophile, hydroxide, on

phosphate triesters with aryloxy leaving groups²⁰ but closer to the β_{lg} values for methoxide attack on diethyl aryl phosphates (-0.70 ± 0.05^{21}), as well as the methoxide (-0.72^{8c}) and hydroxide (-0.69 ,¹⁴ -0.62 , or -0.54^{22}) promoted cyclization of 2-hydroxypropyl aryl phosphates (**1**). Kirby and Younas²³ demonstrated that the attack of oxyanion nucleophiles on methyl aryl phosphate anions can proceed via three competitive pathways involving $\text{CH}_3\text{--OP}$, Ar--OP , and ArO--P cleavage, but the initial rate method used here for monitoring the production of phenoxide or phenol products for all of the substrates except **6a** and **6b** probes the desired reaction proceeding through nucleophilic attack on P.

With **6a** and **6b** product studies show that about 90 and 10% of the respective reactions involve attack on the aryloxy group, from which we can determine the rate constants given in Table 2 for the methoxide attack on P for these substrates. The two open circles on the Brønsted plot of Figure 1 represent the rate constants observed for attack on the aryloxy rings of **6a, b** and the slope of the two point linear regression, $\log k_2^{-\text{OMe}} = (-2.4)_{\text{sp}}K_a + 15.4$, indicates such a large drop in rate with increasing phenol $\text{p}K_a$ that none of the other substrates is expected to encounter competitive methoxide promoted Ar--OP cleavage.

A. Williams suggested some time ago that there is little evidence that acyclic phosphate diesters react with oxyanion nucleophiles by mechanisms other than concerted ones²⁴ and the concerted or synchronous mechanism is supported by heavy atom kinetic isotope effect studies.²⁵ However, there is now good evidence that diesters having β -hydroxy groups capable of acting as intramolecular nucleophiles, such as uridine 3'-phosphate diesters and probably 2-hydroxypropyl phosphates,²⁶ do react via the formation of stable pentacoordinate phosphorane intermediates.²⁷ The β_{lg} value we see here for the methoxide reaction with **6** is consistent with either an associative concerted reaction with little cleavage of the ArO--P bond in the transition state or a two step mechanism with rate limiting formation of a phosphorane intermediate. Williams' charge mapping^{24,28} for the hydrolysis of aryloxy phosphate diesters considers the charges on the starting material and phenolate oxygens are 0.74 and -1.0 in aqueous media. If we assume that these same values obtain for reactions in methanol, as in Scheme 1 we suggest that the methoxide promoted cleavage of **6**, if concerted, is highly associative and has proceeded only 33% of the way along the reaction path leaving a residual charge of $+0.17$ ($0.74\text{--}0.57$)

- (20) Khan, S. A.; Kirby, A. J. *J. Chem. Soc. B* **1970**, 1172.
 (21) Liu, T.; Neverov, A. A.; Tsang, J. S. W.; Brown, R. S. *Org. Biomol. Chem.* **2005**, *3*, 1525.
 (22) Brown, D. M.; Usher, D. A. *J. Chem. Soc.* **1966**, 6558.
 (23) (a) Kirby, A. J.; Younas, M. *J. Chem. Soc. B* **1970**, 1154. (b) Kirby, A. J.; Younas, M. *J. Chem. Soc. B* **1970**, 1165.
 (24) (a) Williams, A. *Concerted Organic and Bio-Organic Mechanisms*; CRC Press: Boca Raton, FL, 2000; pp 161–181. (b) Bourne, N.; Williams, A. *J. Am. Chem. Soc.* **1984**, *106*, 7591. (c) Bourne, N.; Chrystiuk, E.; Davis, A. M.; Williams, A. *J. Am. Chem. Soc.* **1988**, *110*, 1890. (d) Ba-Saif, S. A.; Davis, A. M.; Williams, A. *J. Org. Chem.* **1989**, *54*, 5483.
 (25) (a) Cassano, A. G.; Anderson, V. E.; Harris, M. E. *J. Am. Chem. Soc.* **2002**, *124*, 10964. (b) Hengge, A. C.; Tobin, A. E.; Cleland, W. W. *J. Am. Chem. Soc.* **1996**, *117*, 5919.
 (26) Brown, D. M.; Usher, D. A. *J. Chem. Soc.* **1966**, 6558.
 (27) Lönnberg, H.; Strömberg, R.; Williams, A. *Org. Biomol. Chem.* **2004**, *2*, 2165.
 (28) (a) Williams, A. *Acc. Chem. Res.* **1984**, *17*, 425. (b) Williams, A. *Chem. Soc. Rev.* **1986**, *15*, 125.
 (29) (a) Humphry, T.; Forconi, M.; Williams, N. H.; Hengge, A. C. *J. Am. Chem. Soc.* **2002**, *124*, 14860. (b) Humphry, T.; Forconi, M.; Williams, N. H.; Hengge, A. C. *J. Am. Chem. Soc.* **2004**, *126*, 11864.

(19) Zalatan, J. G.; Herschlag, D. *J. Am. Chem. Soc.* **2006**, *128*, 1293.

Table 3. Kinetic Constants (Maximum Rate Constant ($k_{\text{cat}}^{\text{max}}$), Dissociation Constant (K_{M}), and the Second Order Rate Constant ($k_2^{\text{obs}} = k_{\text{cat}}^{\text{max}}/K_{\text{M}}$) for the Methanolysis of **6a–n** Catalyzed by **3**:Zn(II)₂:⁻OCH₃ at pH 9.8 and 25.0 ± 0.1 °C

phosphate diester	$k_{\text{cat}}^{\text{max}}$ (s ⁻¹) ^a	K_{M} (M) ^a	k_2^{obs} (M ⁻¹ s ⁻¹) ^b	catalytic acceleration at pH 9.8
6a	5.1 ± 0.3	$(3.3 \pm 0.5) \times 10^{-4}$	15000 ± 3000	6.2×10^{11}
6b	0.44 ± 0.01	$(3.2 \pm 0.2) \times 10^{-4}$	1400 ± 200	1.7×10^{12}
6c	0.89 ± 0.09	$(3.7 \pm 0.9) \times 10^{-4}$	2400 ± 600	5.2×10^{12}
6d	0.69 ± 0.03	$(1.7 \pm 0.4) \times 10^{-4}$	4100 ± 200	4.3×10^{12}
6e	$(3.6 \pm 0.4) \times 10^{-2}$	$(2.6 \pm 1.0) \times 10^{-4}$	140 ± 60	4.2×10^{11}
6f	$(4.1 \pm 0.3) \times 10^{-2}$	$(3.7 \pm 0.8) \times 10^{-4}$	110 ± 27	6.1×10^{11}
6g	0.415 ± 0.008	$(3.6 \pm 0.2) \times 10^{-5}$	12000 ± 1000	1.1×10^{13}
6h	0.278 ± 0.006	$(4.5 \pm 0.5) \times 10^{-5}$	6200 ± 100	5.7×10^{12c}
6i	$(1.5 \pm 0.1) \times 10^{-2}$	$(1.8 \pm 0.6) \times 10^{-4}$	83 ± 33	1.0×10^{12}
6j	$(2.9 \pm 0.1) \times 10^{-3}$	$(1.3 \pm 0.2) \times 10^{-4}$	22 ± 4	1.1×10^{12c}
6k	$(7.4 \pm 0.5) \times 10^{-4}$	$(1.4 \pm 0.4) \times 10^{-4}$	5.3 ± 1.9	4.4×10^{11c}
6l	$(3.9 \pm 0.1) \times 10^{-2}$	$(6.9 \pm 0.2) \times 10^{-5}$	570 ± 20	3.3×10^{13c}
6m	$(5.3 \pm 0.3) \times 10^{-4}$	$(2.3 \pm 0.5) \times 10^{-4}$	2.3 ± 0.5	5.3×10^{11c}
6n	$(3.5 \pm 0.1) \times 10^{-4}$	$(1.5 \pm 0.3) \times 10^{-4}$	2.3 ± 0.4	6.2×10^{11c}

^a $k_{\text{cat}}^{\text{max}}$ and K_{M} determined by fits of the k_{obs} vs [Cat] data to eq 1 as described in text. ^b Computed as $k_{\text{cat}}^{\text{max}}/K_{\text{M}}$. ^c Acceleration values for substrates **6h**, **6j–n** were predicted by estimating the k_2^{OMe} values for the base-catalyzed reaction for these less active substrates using the linear regression equation for the Brønsted plot for the base-promoted reaction in Figure 1.

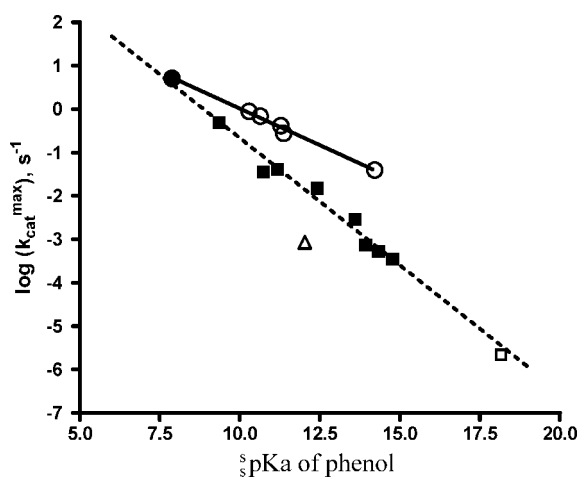
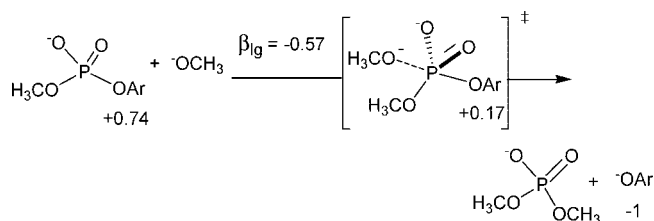


Figure 4. Brønsted plots of $\log(k_{\text{cat}}^{\text{max}})$ vs the $\text{p}K_{\text{a}}$ values for the **3**:Zn(II)₂:⁻OCH₃-catalyzed methanolysis of phosphates **6a**, **c**, **d**, **g**, **h**, and **l** (○) which fits a linear regression of $\log k_{\text{cat}}^{\text{max}} = (-0.34 \pm 0.01) \text{p}K_{\text{a}} + (3.4 \pm 0.2)$; $r^2 = 0.9933$ and phosphates **6b**, **e**, **f**, **i–k**, **m**, and **n** (■) which fits a linear regression of $\log k_{\text{cat}}^{\text{max}} = (-0.59 \pm 0.03) \text{p}K_{\text{a}} + (5.2 \pm 0.4)$; $r^2 = 0.9816$. The datum for methyl 2-*tert*-butyl-4-nitrophenyl phosphate (**7**) (Δ, $k_{\text{cat}} = 8.5 \times 10^{-4} \text{ s}^{-1}$; $\text{p}K_{\text{a}} = 12.03$) sits below both Brønsted lines and that for dimethyl phosphate (□, $k_{\text{cat}} = 2.2 \times 10^{-6} \text{ s}^{-1}$; $\text{p}K_{\text{a}} = 18.16$) rests near the Brønsted line for phosphates that do not include *ortho*-NO₂ or carbomethoxy groups: neither of the latter two points is used to define the linear regression (see text).

Scheme 1. Charge Mapping for a Concerted Displacement of Substrates **6**



still on the aryloxy group in the TS. The difference between the solvation characteristics of methanol and aqueous media could modify the charges on the starting materials somewhat, but the differences are not expected to be large enough to alter the analysis greatly.

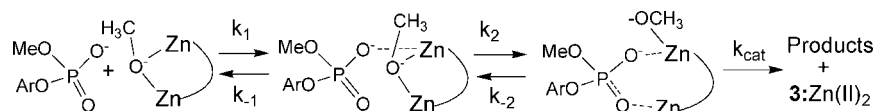
3:Zn(II)₂:⁻OCH₃-Catalyzed Reaction. The complex-catalyzed reactions of all the substrates exhibit consistent saturation

behavior with $k_{\text{cat}}^{\text{max}}$ values spanning 4 orders of magnitude while the corresponding acidity of the leaving group phenols spans 7 orders of magnitude. However, there are two different Brønsted plots in Figure 4 of slopes -0.34 and -0.59 intersecting at the point for methyl 2,4-dinitrophenyl phosphate. The shallower gradient plot incorporates substrates with *ortho*-nitro and carbomethoxy derivatives (**6a**, **c**, **d**, **g**, **h**, **l**) and lies above the steeper gradient plot comprising all other substrates (termed here “regular” substrates). We will deal with these in turn.

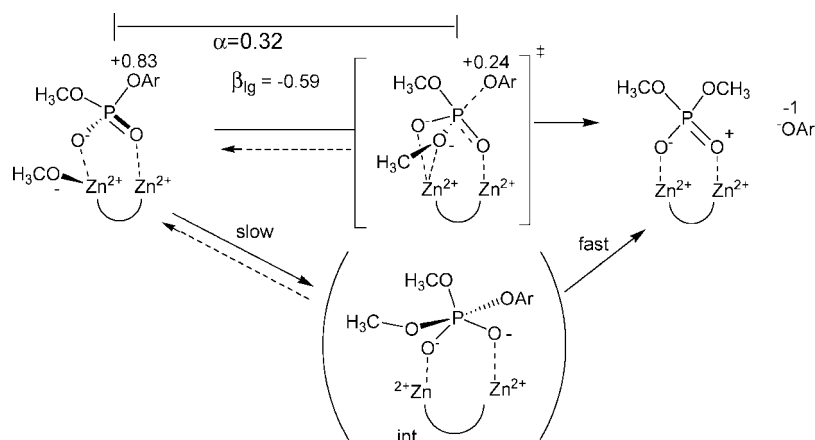
Recent studies of the heavy atom kinetic isotope effect^{29a} on the cleavage of labeled methyl *p*-nitrophenyl phosphates bound to a di-Co(III) complex (**5**), coupled with the β_{lg} of -1.38 reported¹⁴ for the cleavage of four aryl methyl phosphates from various derivatives of **5**, were interpreted^{29a,b} in terms of a two-step mechanism with fast formation of a phosphorane intermediate followed by rate limiting cleavage of the aryloxy leaving group. The β_{lg} of -0.59 for catalyzed transesterification of “regular” substrates **6** suggests a different process is utilized by the **3**:Zn(II)₂:⁻OCH₃ catalyst relative to the di-Co(III) catalyst **5**. Since the general catalytic reaction pathway involving substrate binding and chemical transformation should have common characteristics for related phosphodiester substrates, it is useful to view the results obtained here within the context of three pieces of our earlier work. These are: 1) for **6f** the plot of $k_{\text{cat}}^{\text{max}}$ vs the $[\text{OCH}_3]/[\text{3:Zn(II)}_2]$ ratio is bell-shaped, maximizing at unity,^{8a} suggesting the TS stoichiometry comprises a 1:2:1:1 ratio of ligand, Zn(II), methoxide and substrate; 2) the X-ray diffraction structure^{8c} of the closely related **3**:Zn(II)₂:⁻OH complex shows a hydroxide bridged between the two Zn(II) ions, and this motif is undoubtedly maintained for the methoxide complex in methanol solution, at least prior to substrate binding. The X-ray diffraction structure^{8b} of a related **3**:Cu(II):⁻(OH):((C₆H₅CH₂O)₂PO₂⁻) complex shows that both the dibenzyl phosphate and the hydroxide are bridged between two 5-coordinate metal ions; and 3) the **3**:Zn(II)₂:⁻OCH₃-promoted intramolecular cyclization of a series of 2-hydroxypropyl aryl phosphate diesters (**1**) with aryloxy leaving groups is proposed^{8b,c} to occur by a multistep pathway involving two binding steps and a chemical cleavage step (k_{cat}) which is rate limiting when the corresponding phenol of the aryloxy leaving group has a high $\text{p}K_{\text{a}}$, and very fast (nonrate limiting) when the phenol has a low $\text{p}K_{\text{a}}$.

Substrates **6** react slower than their hydroxypropyl counterparts (~ 5000 -fold for the 4-nitro derivatives) but should follow

Scheme 2. Metal ion charges omitted for simplicity



Scheme 3. Leffler index²⁸ α is Given as $\beta_{lg}/\beta_{eq} = -0.59/-1.83 = 32\%$ and Represents the Extent of the Departure of the OAr Group from the P at the Transition State



the same general process for placement of the substrate into a doubly activated complex as shown in simplified Scheme 2, from which a slower alkoxide mediated cleavage step (k_{cat}) occurs. The products of the reaction are dimethyl phosphate and the corresponding phenol/phenoxide, depending on the ${}^s pK_a$ of the phenol.

i. Methanolysis of Phosphates 6b,e,f,i-k,m and n. The lower Brønsted plot shown in Figure 4 has a β_{lg} of -0.59 ± 0.03 which is essentially the same as that observed for the methoxide reaction, and less than -0.97 ± 0.05 we observed for the k_{cat}^{max} vs ${}^s pK_a$ plot for $3:Zn(II)_2: {}^-OCH_3$ -catalyzed cyclization of the hydroxypropyl aryl phosphates **1**.^{3c} In Scheme 3 are two possible pathways for cleavage of the bound diester within the $3:Zn(II)_2: {}^-OCH_3:6$ complex. Coordination of the phosphate anion to two Zn(II) ions gives the aryloxy oxygen a net positive charge of ~ 0.83 ,^{14,30} similar to that of a phosphate triester. Because it is difficult to envision that a methoxide coordinated between two Zn(II) ions is nucleophilic enough to attack the coordinated phosphate, we propose, as shown in Scheme 3, that one of the bridging methoxide-Zn(II) bonds is broken to allow an intramolecular delivery of the methoxide from a monocoordinated Zn(II)-methoxide, although strictly speaking, the data do not rule out the possibility of attack of an external methoxide³¹ on the $3:Zn(II)_2$ -bound phosphate. If the reaction is concerted, the $\beta_{lg} = -0.59$ suggests the cleavage of the P-aryloxy bond would have progressed only 32% of the way with the oxygen bearing $+0.24$ charge in an associative, but early, TS. An associative mechanism would be greatly enhanced via electrophilic activation by the catalyst through charge removal from the coordinated $(CH_3O)(OAr)PO_2^-$.³² Possibly the stabilization is sufficiently

strong that the reaction is deflected from an associative concerted reaction into a two-step process with rate limiting formation of a phosphorane intermediate (int. in Scheme 3) followed by fast aryloxy anion departure.

ii. Methanolysis of Phosphates 6a,c,d,g,h and i. Also shown in Figure 3 is a second Brønsted plot with $\beta_{lg} = -0.34$ for substrates containing *ortho*-NO₂ or C(=O)OCH₃ groups (but not other *ortho* groups like Cl or *tert*-butyl) which lies above the regression line comprising the “regular” substrates. The rate acceleration due to this *ortho* effect is not small when we compare substrates having similar phenol ${}^s pK_a$ values. For example, the k_{cat}^{max} for substrate **6l** (2-(methoxycarbonyl)phenol, ${}^s pK_a = 14.21$) is 53 and 73 times larger than the respective k_{cat}^{max} terms for substrates **6k** (3-methoxyphenol, ${}^s pK_a = 13.93$) and **6m** (phenol, ${}^s pK_a = 14.33$).

The *ortho* groups in question must bring on some energetically favorable interaction for the catalyzed process and while it is not immediately clear how this is achieved, there are limited possibilities. One involves a different reaction specific to these catalyst-bound substrates involving *ipso*-attack on the ring by an external or internal methoxide to give Ar-OP cleavage and the corresponding anisole product. However, no anisole products could be found (at the limits of detection $\leq 5\%$) for the catalyzed reaction of **6a**, **6g**, and **6m**, the only identifiable products being the phenols resulting from P-OAr cleavage. A second involves a possible general acid catalysis of the leaving group departure by a closely situated Zn(II)-O(H)CH₃ as has been discussed for Zn²⁺(H₂O)_x ion catalysis of RNA model cleavage,³³ although the implication is that any general acid assistance must be unique to the presence of the highly nonbasic *ortho* NO₂ and C(=O)OCH₃ entities. The effect cannot be a simple steric one, since the *o*-chloro derivative shows no deviation from the regular

(30) We assume that binding of a phosphate between two Zn(II) centers has the same net effect as a single protonation based on the observations for the first and second acid dissociation constants of H₂PO₄⁻ bound between two Co(III) centers: Edwards, J. D.; Foong, S.-W.; Sykes, A. G. *J. Chem. Soc., Dalton Trans.* **1973**, 829.

(31) For the fastest substrate (**6a**), the k_{cat}^{max} value is 5 s⁻¹. Attack of free methoxide cannot be ruled out because at ${}^s pH$ 9.8, the $[{}^-OCH_3]$ is 10⁻⁷ M and if it reacts at the diffusion limit of 10¹⁰ M⁻¹ s⁻¹, the upper limit for this reaction would be 1000 s⁻¹.

(32) Patrick, J.; O'Brien, P. J.; Herschlag, D. *Biochemistry* **2002**, *41*, 3207. They present a fine discussion of the ramifications of electrophilic assistance of catalysis via binding of the leaving group to a metal ion in the context of the alkaline phosphatase catalyzed reaction of aryl and alkyl phosphate monoesters.

(33) Mikkola, S.; Stenman, E.; Nurmi, K.; Yousefi-Salakdeh, E.; Strömberg, R.; Lönnberg, H. *J. Chem. Soc., Perkin Trans.* **1999**, *2*, 1619.

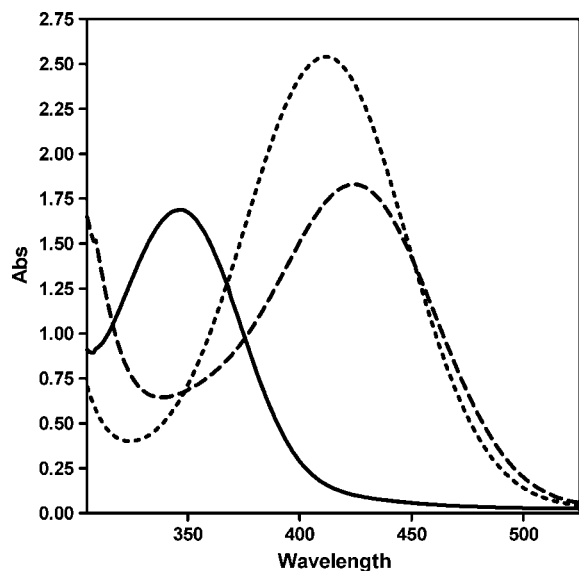


Figure 5. UV spectra in methanol for 0.34 mM 2-nitrophenol (solid line), the corresponding phenoxide (dotted line), and that for the complex of 0.34 mM in each of $3:Zn(II)_2:OCH_3$ and 2-nitrophenol (dashed line).

substrate plot, and the datum point for the *o*-*tert*-butyl derivative (2-*tert*-butyl-4-nitrophenyl methyl phosphate (7)) lies considerably below both lines in Figure 4. Rather, it is more likely that the *o*-NO₂ or C(=O)OCH₃ groups enhance the interaction with the catalyst in a way that decreases the development of negative charge on the departing oxygen, leading to a lower magnitude of β_{lg} due to what might be termed electrophilic assistance or possibly second-sphere coordination³⁴ that enhances increased ion-dipole interaction, hydrogen bonding or hydrophobic interaction between catalyst and transforming substrate in the TS. Electrophilic assistance of the departure of aryloxy leaving groups via general acid assistance has been proposed to explain the low β_{lg} observed for the cleavage of uridine-3'-phosphate aryl esters promoted by bovine pancreatic RNase A³⁵ and more recently to explain the rapid cleavage of methyl 8-dimethylamino-1-naphthyl phosphate with a variety of nucleophiles under acidic conditions where intramolecular general acid assistance plays a key role.³⁶

The UV/vis spectra of the corresponding *o*-substituted phenols show evidence of an enhanced binding to the $3:Zn(II)_2:OCH_3$ complex which is not seen for phenols having similar ${}^s pK_a$ values but no *o*-substituent. In Figure 5 are displayed spectra of 2-nitrophenol, its phenoxide and that of 2-nitrophenol in the presence of $3:Zn(II)_2:OCH_3$. The latter shows a new band from the phenol or phenoxide which can only arise from a higher order phenoxide: $3:Zn(II)_2:OCH_3$ interaction. Similar sets of spectra are generated with 2,4-dinitrophenol, and 2-carbomethoxyphenol, suggesting that these two *o*-substituted phenols are also deprotonated and form higher order complexes with $3:Zn(II)_2:OCH_3$. This is not the case with 4-nitrophenol as its UV/vis spectrum does not change in the presence of $3:Zn(II)_2:OCH_3$ (see Supporting Information).

Although the above refers specifically to the phenol product with $3:Zn(II)_2:OCH_3$, there is weak indication from the K_M

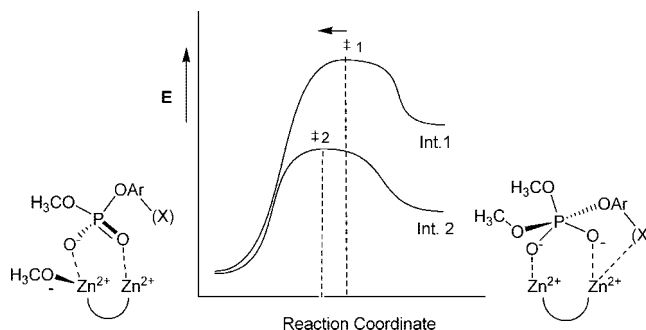


Figure 6. Reaction coordinate diagram for the formation of a phosphorane/di-Zn(II) stabilized complex (Int.1) without the extra binding stabilization of the *ortho*-group X; and (Int.2) with the extra binding stabilization of the *ortho*-group X showing the shift of the TS to the left.

values given in Table 3 that the *o*-substituted substrates (e.g., **6g**, **6h**, **6l**) do bind somewhat tighter to the catalyst in the ground state, but of course in order to produce an increase in reaction rate the rate-limiting transition state would have to bind tighter yet³⁷ due to the proposed electrophilic assistance or second-sphere coordination. According to the reaction coordinate diagram shown in Figure 6, such additional stabilization of the phosphorane complex shifts the TS to the left with less weakening of the P---OAr bond and less charge neutralization on the aryloxy group, leading to a less negative Brønsted β_{lg} as observed.

Our proposed mechanism of a catalyzed two-step reaction involving rate-limiting formation of a $3:Zn(II)_2$ complexed phosphorane intermediate invites comparison with two earlier model studies of the hydrolysis of aryl methyl phosphates mediated by Co(III) complexes **4** and **5**. For the dinuclear Co(III) complexed phosphate diesters (**5**),¹⁴ the data are consistent with a two-step reaction with fast formation a phosphorane intermediate followed by slow expulsion of the aryloxy leaving group to form a highly strained di-Co(III) complexed phosphate having two conjoined four-membered rings. Formation of a highly strained product requires an increased cleavage of the P---OAr bond in the TS accounting for the large negative β_{lg} value of -1.38 .¹⁴ An important consequence of the large Brønsted β_{lg} relative to that for the hydroxide promoted reaction (-0.64),¹⁴ is that catalyzed cleavage of substrates with good leaving groups is much more effective than for substrates with poor leaving groups.

In the second case of the hydrolysis of a series of **6** promoted by **4**, N. Williams and co-workers¹³ surmised that the most probable mechanism involved two steps with an intramolecular attack of a Co(III)-OH on a transiently coordinated phosphate. That the observed Brønsted β_{lg} changed from -0.17 to -1.05 at a $pK_{a(lg)}$ of ~ 6 is consistent with a change in mechanism from rate limiting formation of a phosphorane intermediate with good leaving groups to breakdown with poorer ones. This interpretation would be consistent with what we observe, with the important modification that there is no break in the Brønsted plots that would signify a change in the rate limiting step to breakdown over the ${}^s pK_a$ range encompassed by the substrates used here. We suggest that the smaller β_{lg} of -0.59 (or -0.34 in the case of the *ortho*-substrates) observed for the $3:Zn(II)_2:OCH_3$ catalyzed reaction is most consistent with a two step

(34) Raymo, F. M.; Stoddart, J. F. *Chem. Ber.* **1996**, *129*, 981.

(35) Davis, A. M.; Regan, A. C.; Williams, A. *Biochemistry* **1988**, *27*, 9042.

(36) Kirby, A. J.; Lima, M. F.; Da Silva, D.; Roussev, C. D.; Nome, F. *J. Am. Chem. Soc.* **2006**, *128*, 16944.

(37) (a) Jencks, W. P. *Catalysis in Chemistry and Enzymology*; Dover Publications: New York, 1987. (b) Wolfenden, R. *Acc. Chem. Res.* **1972**, *5*, 10. (c) Lienhard, G. E. *Science* **1973**, *180*, 149.

Table 4. ($k_{\text{cat}}/K_{\text{M}}/K_{\text{a}}/K_{\text{w}}$) and ($k_{\text{cat}}/K_{\text{M}}/k_2^{-\text{OMe}}$) Constants and Computed Free Energies of Formation of Michaelis Complex ($\Delta G_{\text{Bind}} - \Delta G_{\text{M}}$), the Free Energies of Activation for k_{cat} ($\Delta G_{\text{cat}}^{\ddagger}$), and the Free Energies of Stabilization of the Methoxide Transition State through Binding to $3:\text{Zn}(\text{II})_2$ ($\Delta\Delta G_{\text{stab}}$) for the Reaction of $3:\text{Zn}(\text{II})_2 \cdot \text{OCH}_3$ with Substrates **6a–n** at 25.0 ± 0.1 °C in Methanol^{a,b}

substrate	$(k_{\text{cat}}/K_{\text{M}})/k_2^{-\text{OMe}}$	$(k_{\text{cat}}/K_{\text{M}})(K_{\text{a}}/K_{\text{w}})$ ($\text{M}^{-2} \text{s}^{-1}$) ^{c,d}	$\Delta G_{\text{Bind}} - \Delta G_{\text{M}}$ (kcal/mol) ^e	$\Delta G_{\text{cat}}^{\ddagger}$ (kcal/mol) ^f	$\Delta G_{\text{Non}}^{\ddagger}$ (kcal/mol) ^f	$\Delta\Delta G_{\text{stab}}^{\ddagger}$ (kcal/mol)
6a	1.94×10^8	3.43×10^{11}	-14.8	16.4	23.0	-21.4
6b	5.8×10^8	3.2×10^{10}	-14.8	17.9	25.1	-22.0
6c	1.2×10^9	5.5×10^{10}	-14.7	17.5	25.2	-22.4
6d	2.2×10^9	9.4×10^{10}	-15.1	17.6	25.2	-22.7
6e	1.4×10^8	3.2×10^9	-14.9	19.4	25.6	-21.1
6f	1.4×10^8	2.5×10^9	-14.7	19.3	25.7	-21.1
6g	3.3×10^{10}	2.5×10^{11}	-16.1	17.9	26.2	-24.4
6h	1.3×10^{10}	1.4×10^{11}	-16.0	18.1	26.1	-24.0
6i	5.9×10^8	1.9×10^9	-15.1	19.9	26.8	-22.0
6j	9.2×10^8	5.3×10^8	-15.3	20.9	27.8	-22.2
6k	3.4×10^8	1.3×10^8	-15.3	21.7	28.0	-21.6
6l	5.2×10^{10}	1.3×10^{10}	-15.7	19.5	28.3	-24.5
6m	2.4×10^7	5.3×10^7	-15.0	21.9	28.4	-21.5
6n	4.3×10^7	5.3×10^7	-15.2	22.1	28.7	-21.8

^a Italicized numbers are for *o*-NO₂ and C(=O)OCH₃ derivatives. ^b $\Delta G_{\text{stab}}^{\ddagger}$ computed from application of kinetic and equilibrium constants to eq (2); $k_2^{-\text{OMe}}$ constants from Table 2. ^c $k_{\text{cat}}/K_{\text{M}}$ from Table 3. ^d K_{a} determined from half-neutralization^{3b} to be $10^{-9.41}$; $K_{\text{w}} = 10^{-16.77}$; $K_{\text{a}}/K_{\text{w}} = 2.3 \times 10^7$. ^e Computed as $(\Delta G_{\text{Bind}} - \Delta G_{\text{M}}) = -RT \ln((K_{\text{a}}/K_{\text{w}})/K_{\text{M}})$. ^f Computed from $\Delta G_{\text{cat}}^{\ddagger} = -RT \ln(k_{\text{cat}}/(kT/h))$ or $\Delta G_{\text{Non}}^{\ddagger} = -RT \ln(k_2^{-\text{OMe}}/(kT/h))$ from the Eyring equation where $(kT/h) = 6 \times 10^{12} \text{ s}^{-1}$ at 298 K.

process with rate limiting formation of the phosphorane intermediate. The fast departure of the leaving group in our case, but not with **4** or **5**, perhaps results from a conformational flexibility of $3:\text{Zn}(\text{II})_2$, not seen with the Co(III) complexes, that accommodates the transforming substrate while it passes along the reaction coordinate, electrostatically stabilizing the phosphorane intermediate, its formation, pseudorotation and its breakdown, and also complementing the substrate's geometric changes in passing between four- and five-coordinate phosphorus.

For $3:\text{Zn}(\text{II})_2 \cdot \text{OCH}_3$ reacting with the “regular” substrates **6**, the Brønsted β_{lg} of -0.59 (Figure 4) is the same as observed for the methoxide reaction for the eight most rapidly reacting substrates ($\beta_{\text{lg}} = -0.57$, Figure 1). This indicates that substrates with both good and poor leaving groups will be catalyzed to the same extent, at least for the “regular” substrates. More importantly, the smaller β_{lg} of -0.34 observed for the catalyzed reaction of the group of *ortho*-nitro- and carbomethoxy-substituted substrates indicates that this catalyst promotes the cleavage of substrates with poorer leaving groups more than ones with better leaving groups, bearing in mind our categorization of the leaving group ability is based solely on phenol $\text{p}K_{\text{a}}$.

iii. Catalyzed Methanolysis of Dimethyl Phosphate. On the lower Brønsted plot in Figure 4 is a point (\square) for $(\text{CH}_3\text{O})_2\text{PO}_2^-$ determined for 0.9 mM dimethyl phosphate reacting with 1.0 mM $3:\text{Zn}(\text{II})_2 \cdot \text{OCD}_3$ in CD_3OD at ambient temperature, pH 9.8. This was determined from quantitative mass analysis of the recovered dimethyl phosphate for the intensities of the M^+ and $(\text{M}^+ + 3)$ peaks checking for the replacement of OCH_3 with OCD_3 .³⁸ The observed rate constant (k_{cat}) for formation of $(\text{CH}_3\text{O})(\text{CD}_3\text{O})\text{PO}_2^-$, corrected for an incomplete binding of substrate and statistically for the expulsion of CH_3O vs CD_3O from a putative phosphorane intermediate, is $(2.27 \pm 0.03) \times 10^{-6} \text{ s}^{-1}$ or $t_{1/2} = 85 \text{ h}$ which compares favorably with a k_{cat} of $(9 \pm 3) \times 10^{-6} \text{ s}^{-1}$ reported for the transesterification of dimethyl phosphate catalyzed by a di-Cu(II) complex in CD_3OD at 25 °C.^{11,39}

The fact that dimethyl phosphate fits very near the Brønsted line of $\beta_{\text{lg}} -0.59$ derived from the $\log k_{\text{cat}}$ vs $\text{p}K_{\text{a}}$ data for “regular” phosphates⁴⁰ provides some evidence that the mechanism for its catalyzed cleavage is the same as that for the

methyl aryl phosphates even though the leaving groups are substantially different. There are at least four possible processes consistent with the observations, namely whether the attacking methoxide is external, or metal-coordinated, and whether the reaction is concerted or two-step, although for the reasons reiterated previously, we favor (although not rigidly so) the metal-coordinated methoxide proceeding through a two step process with rate limiting formation of the phosphorane. For such a symmetrical reaction occurring via a metal-delivered methoxide, microscopic reversibility requires that methoxide departure must also be metal-promoted. Thus, the five-coordinate intermediate must be geometrically mobile enough that pseudorotation and methoxide interchange on the Zn(II) cannot limit the rate. For that process, and a mechanism involving an external nucleophile proceeds via two steps, one anticipates a gradual change in the rate limiting step from formation to breakdown of the 5-coordinate intermediate. That the datum point for dimethyl phosphate lies slightly below the extrapolated line may signify that there is the onset of the anticipated break attributable to the expected change in rate limiting step, but more study with several additional derivatives having poor leaving groups is required before this can be confirmed.

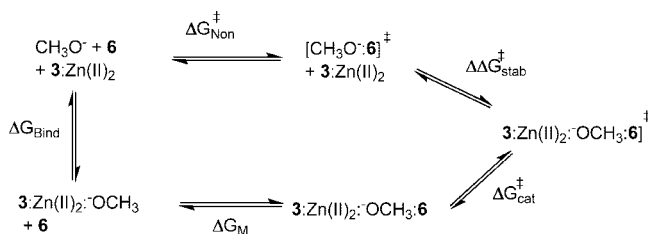
iv. Energetics Associated with the Catalyzed Reaction. The acceleration afforded by $3:\text{Zn}(\text{II})_2 \cdot \text{OCH}_3$ (or a chemical equivalent such as $3:\text{Zn}(\text{II})_2 + (\text{OCH}_3^-)$) in cleaving **6** can be judged in comparison with the CH_3O^- -promoted reaction. Relative to the $k_2^{-\text{OMe}}$ values given in Table 2 for substrates **6a–g,i**, the catalytic second order rate constants (given as $k_2^{\text{obs}} = k_{\text{cat}}^{\text{max}}/K_{\text{M}}$ in Table 4) are larger by 1.4×10^8 to 3×10^9 -fold, the substrates with *ortho*-NO₂ or C(=O)OCH₃ groups (**6b,c,g**) exhibiting the largest enhancements. These realistically have errors of $\pm 20\%$ due to the relatively low accuracy placed on the K_{M} dissociation constants as well as the $k_2^{-\text{OMe}}$ values determined for the slow methoxide reactions, but such errors do not detract in any major way from the significant enhance-

(38) Melnychuk, S. A.; Brown, R. S. unpublished results. For experimental details pertaining to this experiment, see Supporting Information.

(39) The dinuclear Cu(II) catalyst reported in ref 11 is indeed unusual because it is reported to transesterify the CH_3O group dimethyl phosphate at 50 °C about 6 times faster than it does the CH_3O group of methyl-*p*-nitrophenyl phosphate (**6f**) and about 5.5 times faster than it cleaves the *p*-nitrophenoxy group of the latter. We do not see this phenomenon with $3:\text{Zn}(\text{II})_2 \cdot \text{OCH}_3$.

(40) A β_{lg} of -0.60 is computed when all data points for “regular” methyl aryl phosphates and that for dimethyl phosphate are considered.

Scheme 4



ment provided by $3:\text{Zn}(\text{II})_2:\text{OCH}_3$. An alternative comparison of the $k_{\text{cat}}^{\text{max}}$ observed for the bound substrates **6a–g,i** with the pseudofirst order rate constant calculated from the methoxide $k_2^{-\text{OMe}}$ at the pH where the catalyst is active (9.8) gives accelerations ranging from 4×10^{11} to 1×10^{13} . The latter accelerations provided for the DNA model substrates compare favorably with the 1×10^{12} to 4×10^{12} accelerations previously obtained^{8c} for the intramolecular transesterification of a series of RNA models (2-hydroxypropyl aryl phosphates) in methanol, although in that study none of the special *ortho*-substrates was studied.

A revealing way of assessing catalytic efficacy quantifies the free energy difference between the transition state for the methoxide reaction of **6** ($\text{CH}_3\text{O}^-:\text{6}$)[‡] and a catalytic transition state comprising $3:\text{Zn}(\text{II})_2:\text{OCH}_3$ plus **6** (or any of its kinetic equivalents such as $3:\text{Zn}(\text{II})_2 + \text{OCH}_3 + \text{6}$). This comparison, widely used for comparing enzyme and man-made catalyst-promoted reactions relative to background reactions,^{41,42} proved very useful in a recent analysis of the origin of the acceleration afforded by $3:\text{Zn}(\text{II})_2:\text{OCH}_3$ to transesterification of 2-hydroxypropyl aryl phosphates **1** and **6f**.^{8c,b} Shown in Scheme 4 is a thermodynamic cycle involving both the methoxide reaction and the $3:\text{Zn}(\text{II})_2:\text{OCH}_3$ promoted (or kinetically equivalent) reactions of **6a–m** for which eq 2 provides the stabilization free energy ($\Delta\Delta G_{\text{stab}}^{\ddagger}$) difference between $[3:\text{Zn}(\text{II})_2:\text{OCH}_3:\text{6}]^{\ddagger}$ and $[\text{CH}_3\text{O}^-:\text{6}]^{\ddagger}$. The analysis and definition of terms is identical with the treatments given previously^{8b,c} and need not be repeated here.

$$\Delta\Delta G_{\text{stab}}^{\ddagger} = (\Delta G_{\text{Bind}} - \Delta G_{\text{M}} + \Delta G_{\text{cat}}^{\ddagger}) - \Delta G_{\text{Non}}^{\ddagger} = -RT \ln \times \left[\frac{(k_{\text{cat}}/K_{\text{M}})(K_{\text{a}}/K_{\text{w}})}{k_2^{-\text{OMe}}} \right] \quad (2)$$

The $k_2^{-\text{OMe}}$ values and $k_{\text{cat}}/K_{\text{M}}$ values in eq 2 are from Tables 2 and 3 respectively and for slow reactions where the experimental $k_2^{-\text{OMe}}$ values are not available, these are estimated (without error limits) from the Brønsted relationship $k_2^{-\text{OMe}} = -0.57 \text{p}K_{\text{a}} + 0.14$. Listed in Table 4 are the $(k_{\text{cat}}/K_{\text{M}})/k_2^{-\text{OMe}}$ and $(k_{\text{cat}}/K_{\text{M}})(K_{\text{a}}/K_{\text{w}})$ constants and computed $\Delta\Delta G_{\text{stab}}^{\ddagger}$ values

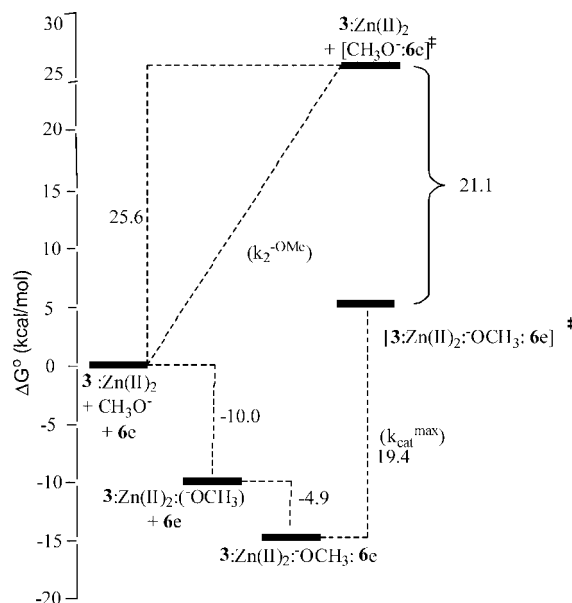


Figure 7. Activation energy diagram for the reaction of CH_3O^- and $3:\text{Zn}(\text{II})_2:\text{OCH}_3$ with substrate **6e** at standard state of 1 M and $T = 25.0 \pm 0.1$ °C showing the calculated energies of binding of the methoxide by $3:\text{Zn}(\text{II})_2$, of binding of the substrate to $3:\text{Zn}(\text{II})_2:\text{OCH}_3$, and the calculated activation energies associated with k_{cat} and $k_2^{-\text{OMe}}$.

which fit into a narrow range of -21 to -22 kcal/mol for the ‘regular’ substrates without the *ortho*- NO_2 or $\text{C}(=\text{O})\text{OCH}_3$ substituents and a more expanded range of -22.4 to -24.5 kcal/mol for the *ortho*-substituted substrates. This is as expected from the Brønsted plots shown in Figures 1 and 4 which have essentially identical slopes of ~ -0.57 and -0.59 for the methoxide and catalyzed reactions of the substrates with no *ortho* substituents, so it is expected that the overall $\Delta\Delta G_{\text{stab}}^{\ddagger}$ for these substrates will not change appreciably with $\text{p}K_{\text{a}}$. However the shallower Brønsted plot in Figure 4 for the catalyzed reactions of the *o*- NO_2 and $\text{C}(=\text{O})\text{OCH}_3$ substituted substrates means that the $\Delta\Delta G_{\text{stab}}^{\ddagger}$ should become increasingly negative with increasing substrate $\text{p}K_{\text{a}}$. Further dissection indicates that the $K_{\text{a}}/K_{\text{w}}$ term contributes -10.0 kcal/mol to the $\Delta\Delta G_{\text{stab}}^{\ddagger}$ for all substrates, while the $(k_{\text{cat}}/K_{\text{M}})/k_2^{-\text{OMe}}$ terms, pertaining to the apparent second order rate constant for the catalytic reaction relative to the methoxide reaction, contribute a somewhat larger and variable amount (-10.0 to -14.6 kcal/mol), with the largest negative numbers being for the substrates with high phenol $\text{p}K_{\text{a}}$ values that also contain the *o*- NO_2 or $\text{C}(=\text{O})\text{OCH}_3$ substituents. A small contribution comes from the K_{M} values which fall into a narrow range of -4.7 to -6.0 kcal/mol, with the larger negative numbers generally belonging to substrates with *o*- NO_2 or $\text{C}(=\text{O})\text{OCH}_3$ substituents.

The $\Delta\Delta G_{\text{stab}}^{\ddagger}$ for the catalyzed reaction of dimethyl phosphate can be estimated from the experimental data only if we extrapolate a value for its methoxide reaction⁴³ of $3.2 \times 10^{-11} \text{M}^{-1}\text{s}^{-1}$ from the Brønsted relationship in Figure 1, and assume a K_{M} value of $2 \times 10^{-4} \text{M}$ from the average of the experimental values for the ‘regular’ phosphate (Table 3). With these values, the $\Delta\Delta G_{\text{stab}}^{\ddagger}$ is -21.7 kcal/mol.

The energies associated with the various components of the thermodynamic cycle shown in Scheme 3 are easily appreciated via visualization of the activation energy diagram exemplified for the reaction of **6e** in Figure 7. At a standard state of 1 M, methoxide attack has a $\Delta G_{\text{non}}^{\ddagger}$ of 25.6 kcal/mol. For the

(41) Wolfenden, R. *Nature* **1969**, 223, 704.

(42) For analyses of this treatment, see: Yatsimirsky, A. K. *Coord. Chem. Rev.* **2005**, 249, 1997, and references therein.

(43) The rate constant for methoxide attack on the P of dimethyl phosphate (DMP) is not known but might be estimated from the extrapolation of the Brønsted plot as described in the text, or from literature work as follows: Guthrie, J. P., *J. Am. Chem. Soc.* **1977**, 99, 3991, has computed the bimolecular rate constant for hydroxide attack on DMP at 25 °C in water of $6.8 \times 10^{-12} \text{M}^{-1}\text{s}^{-1}$. On the other hand, from the extrapolation of high temperature data, Williams and Wyman (Williams, N. H.; Wyman, P. *Chem. Commun.* **2001**, 1268) have determined that a di-neopentyl type phosphate diester (*bis*(2,2-dimethyl-3-(*p*-carboxyphenyl)propyl) phosphate) reacts with HO^- with a rate constant of $1 \times 10^{-15} \text{M}^{-1}\text{s}^{-1}$.¹ Where comparisons can be made,^{6–8} the attack of methoxide on diesters in methanol is only slightly less (a factor of 2–4) than those reported for attack of HO^- on phosphate diesters in water, so the above two rate constants might be considered as limits for the reaction of CH_3O^- on P

catalyzed process, preliminary binding of both methoxide and substrate to the catalyst is accompanied by a reduction in free energy of -14.9 kcal/mol. The $\Delta G_{\text{cat}}^{\ddagger}$ of 19.4 kcal/mol computed for k_{cat} brings the activated complex of $[3:\text{Zn}(\text{II})_2:\text{OCH}_3:6\text{e}]^{\ddagger}$ to a level that is -21.1 kcal/mol lower than the transition state for the methoxide reaction.

Conclusions

The catalysis of the cleavage of the **6a–n** and dimethyl phosphate brought about by a simple system comprising $3:\text{Zn}(\text{II})_2:\text{OCH}_3$ and a medium effect provided by the methanol solvent stands out among all known catalytic systems for the cleavage of a well-defined series DNA models. A recent report¹⁹ of alkaline phosphatase (AP) catalyzed hydrolysis of a series of methyl aryl phosphates that included several of the substrates studied here (**6f, i, j, m**), gave $k_{\text{cat}}/K_{\text{M}}$ values 230–880-fold smaller than what we find for the methanolysis promoted by the $3:\text{Zn}(\text{II})_2:\text{OCH}_3$. Of course the natural substrates for AP are phosphate monoesters for which the catalyzed reactions are $\sim 10^{17}$ -fold faster than the solution reaction, but the 10^{11} -fold overall rate enhancement observed for AP promoted diester hydrolysis relative to the solution reaction¹⁹ is substantial. In the present case, $3:\text{Zn}(\text{II})_2:\text{OCH}_3$ accelerates the methanolytic cleavage of the methyl aryl phosphate diesters by factors of between 4×10^{11} and 3×10^{13} relative to the solution reaction at pH 9.8.

The available data are consistent with a mechanism for the chemical cleavage involving a two step process with rate-limiting formation of a phosphorane intermediate or, less likely in our opinion, an associative concerted process with little cleavage of the aryloxy leaving group in the transition state. It is interesting that the same catalyst also promotes the cyclization of a series of 2-hydroxypropyl aryl phosphates with rate accelerations very similar to what we see here for a quite different reaction involving a nucleophilic attack of methoxide on a phosphate doubly activated by $\text{Zn}(\text{II})\text{---O---P---O---Zn}(\text{II})$ coordination. Whether the reaction involves an external methoxide or intramolecular delivery of metal-coordinated methoxide cannot be ascertained from the kinetics, but intuitively we favor the latter for its chemical efficiency wherein all the catalytically required components ($3:\text{Zn}(\text{II})_2$, substrate and OCH_3) are recruited into one higher order complex prior to initiating the chemical cleavage step.⁴⁴

An essential component of the very high catalytic rates we see in methanol must arise from the medium effect. It is likely that enzyme active sites comprise a domain of effectively reduced dielectric constant decorated with oriented functional groups to create a specific medium, or what we can term a "molecular bottle", tailored for a given reaction.⁴⁵ Because

$3:\text{Zn}(\text{II})_2$ is a poor catalyst for the cleavage of phosphate diesters in water,⁴⁶ but is an exceptionally good one in methanol, it seems that the net positively charged catalyst is an important, but not exclusive, component probably acting electrostatically to assemble and orient the reaction partners and subsequently escort the transforming anionic substrate through a low energy path along the reaction coordinate. To exert its maximum catalytic effect, this system requires an intimately associated low dielectric constant/polarity environment that appears to be satisfied by light alcohols such as methanol.

It has been pointed out^{3g} that enzymes that promote the cleavage of phosphodiester^{1,9} provide ~ 20 to 23 kcal/mol of stabilization energy to the transition state of the catalyzed reaction relative to that of the background reaction. In the present case, the $\Delta\Delta G_{\text{stab}}^{\ddagger}$ of -21 to -24 kcal/mol for $3:\text{Zn}(\text{II})_2:\text{OCH}_3$ promoted cyclization of substrates **6** in methanol approaches that exhibited by such efficient enzymes, bearing in mind the solvent differences for the enzymatic and small molecule catalyst studied here. The present model system also exhibits an interesting enhanced catalysis of *o*-NO₂ and C(=O)OCH₃ substrates that suggests that an improvement in efficiency might be realized in a situation where there is an energetically favorable interaction between the catalyst and the leaving group of the phosphodiester. A most important part of these observation is the reduced gradient for the Brønsted plot for these *ortho*-substituted derivatives which predicts that those substrates with poorer leaving groups (as judged by the $\text{p}K_{\text{a}}$ value for the corresponding phenol) are more effectively cleaved by the catalyst relative to the methoxide background reaction. These observations suggest that one should be able to design transition metal ion complexes that enhance the cleavage of substrates having leaving groups with a built-in additional affinity for the catalyst.

Acknowledgment. We gratefully acknowledge the financial assistance of the Natural Sciences and Engineering Research Council of Canada (NSERC), The Canada Council of the Arts (CCA), and the Canada Foundation for Innovation (CFI). We are indebted to Prof. Jik Chin for helpful discussions. In addition, S.E.B. thanks NSERC for an Undergraduate Summer Research Award, C.T.L. thanks NSERC for a PGS-2 postgraduate scholarship, and R.S.B. thanks the CCA for a Killam Research Fellowship, 2007–2009. Finally, we are indebted to Dr. Y.-M. She of the Mass Spectrometry Facility at Queen's University for his expertise in determining the mass spectra of the product mixtures resulting from the catalyzed methanolysis of dimethyl phosphate.

Supporting Information Available: Tables of pseudofirst order rate constants for reactions of **6a–n** with $3:\text{Zn}(\text{II})_2:\text{OCH}_3$; NMR and mass spectroscopic data for the identity of substrates **6a–n**; UV/vis spectra for various *ortho*-substituted phenols in the presence of $3:\text{Zn}(\text{II})_2:\text{OCH}_3$; mass spectrometric data for the catalyzed methanolysis of dimethylphosphate in CD₃OD promoted by $3:\text{Zn}(\text{II})_2:\text{OCD}_3$; (25 pages). This material is available free of charge via the Internet at <http://pubs.acs.org>.

JA8006963

(44) When a solution containing 1 mM of $3:\text{Zn}(\text{II})_2:\text{OCH}_3$ (measured pH = 9.8) is treated with 0.9 mM of dimethyl phosphate, the measured pH is 9.5, signifying that the methoxide originally attached to the catalyst is retained when it is bound to the phosphate: Edwards, D.; Brown, R. S. , Unpublished observations.

(45) Richard, J. P.; Ames, T. L. *Bioorg. Chem.* **2004**, *32*, 354.

(46) Kim and Lim (ref 16) have reported that the cleavage of *bis*(2,4-dinitrophenyl) phosphate promoted by $3:\text{Zn}(\text{II})_2$ in water as a function of pH is not markedly different from the catalysis afforded by the mono $\text{Zn}(\text{II})$ complex of 1,5,9-triazacyclododecane, the rate constant for the former being $7 \times 10^{-3} \text{ M}^{-1} \text{ s}^{-1}$ at pH 7.